



**HAL**  
open science

# Reshaping plasmonic resonances using epsilon-near-zero materials for enhanced infrared vibrational spectroscopy

Rafik Smaali, Thierry Taliercio, Antoine Moreau, Emmanuel Centeno

## ► To cite this version:

Rafik Smaali, Thierry Taliercio, Antoine Moreau, Emmanuel Centeno. Reshaping plasmonic resonances using epsilon-near-zero materials for enhanced infrared vibrational spectroscopy. *Applied Physics Letters*, 2021, 119, 10.1063/5.0070748 . hal-04042310

**HAL Id: hal-04042310**

**<https://hal.science/hal-04042310>**

Submitted on 23 Mar 2023

**HAL** is a multi-disciplinary open access archive for the deposit and dissemination of scientific research documents, whether they are published or not. The documents may come from teaching and research institutions in France or abroad, or from public or private research centers.

L'archive ouverte pluridisciplinaire **HAL**, est destinée au dépôt et à la diffusion de documents scientifiques de niveau recherche, publiés ou non, émanant des établissements d'enseignement et de recherche français ou étrangers, des laboratoires publics ou privés.

## Reshaping plasmonic resonances using epsilon-near-zero materials for enhanced infrared vibrational spectroscopy

Rafik Smaali,<sup>1</sup> Thierry Taliercio,<sup>2</sup> Antoine Moreau,<sup>1</sup> and Emmanuel Centeno<sup>1, a)</sup>

<sup>1</sup>Université Clermont Auvergne, CNRS, SIGMA Clermont, Institut Pascal, F-63000 Clermont-Ferrand, France

<sup>2</sup>IES, Univ Montpellier, UMR CNRS 5214, Montpellier, FR

(Dated: 14 October 2021)

Surface-enhanced infrared absorption (SEIRA) spectroscopy is a powerful technique for a label-free identification of molecular species. The low infrared absorption cross sections of molecules are made up for the huge electromagnetic field enhancement provided by the resonant excitation of collective electron oscillations in metallic nanoantennas. Since these surface plasmons are localized at nanometer scale, a minute amount of material is detected leading to a weak SEIRA signal. The design of actual plasmonics detectors is a trade off between the detection of very small volumes of molecules and the signal to noise ratio level. We demonstrate that an epsilon-near-zero (ENZ) material combined with nano-slits lifts this constraint and provides both extreme enhancement factor up to  $10^7$  and highly contrasted SEIRA signal for an extremely low amount of material of interest. These results are explained by the modification of the electromagnetic field of the gap plasmon mode sustained by the slits in presence of the ENZ material. We propose to implement this concept with a semiconductor whose doping level engineering provides a versatile way to scan the whole molecules' fingerprint frequency range.

Infrared (IR) absorption spectroscopy is a label-free technique giving access to the vibrational fingerprints of molecules<sup>1</sup>. However, the small IR absorption cross-section of molecules prevents an efficient coupling to long-wavelength mid-IR radiations, resulting in a weak mid-IR absorption signal. Surface-enhanced infrared absorption (SEIRA) is a powerful method to address this issue. The optical absorption of the molecules is enhanced by the excitation of a surface plasmon localized at the surface of a metallic structures<sup>2,3</sup>. The engineering of metallic substrates has thus constituted a way to increase the electromagnetic confinement of plasmonic waves and consequently the strength of the SEIRA signal<sup>4</sup>.

It presently seems however that any design for a sensor based on metallic nanostructures is a trade off between (i) the Enhancement Factor (EF), defined as the ratio of the SEIRA signals with and without structuring normalized by the effective detection zone, (ii) the signal to noise ratio, directly linked to size of the detection zone and, (iii) the spectral selectivity of the device.

Concentrating light into a deeply subwavelength volume allows to reach very high enhancement factors – but this often simply means that the detection zone is extremely small, contains only a few molecules, and thus that the signal to noise ratio is very low<sup>5-9</sup>. The best example are bowtie-shaped antenna, structures with a relatively large footprint which present an extreme EF up to  $10^7$  but can detect only molecules which are trapped in the tiny gap in the structure<sup>10</sup>. Increasing the volume of the detection zone allows to enhance the signal emitted by many more molecules, which leads to a satisfying signal to noise ratio but typically to lower enhancement factors. Several geometries such as disk or strips, U-shape cavities and coaxial apertures of nanometric gap have

been investigated to reconcile a large detection zone and a high EF ( $10^4 - 10^5$ ),<sup>11-14</sup>

Finally, whereas the fingerprint of a given molecule may extend over a large IR range, plasmonic resonances appear way too narrow to be able to cover the entirety of the desired spectrum. The design of the plasmonic nanostructure has to be adapted leading to an increased complexity.<sup>15</sup>

For several different reasons, nanoslits may well be the kind of plasmonic structure with the most potential as plasmonic sensor. They clearly outperform nanorods, their complementary structure,<sup>16</sup> and lead to structures with unprecedented field confinement capabilities due to a very large cross section.<sup>17,18</sup> Nanoslits support a plasmonic mode called *gap-plasmon* that provides an extreme sub-wavelength light confinement and consequently a strong light-matter interaction.<sup>19,20</sup> In addition, bringing molecules of interest inside the slits is doable, for some geometries. However, the electric field hot spots are often located at the edges of the slits and not in the whole volume, which does not allow to escape the above mentioned trade-off. Nanoslit-based devices offer a relatively large detection zone and thus decent signal to noise ratio but enhancement factors of at most  $10^5$ .

It has been recently shown that Epsilon-Near-Zero (ENZ) materials may assist the enhanced transmission through sub-wavelength slits because they help the incoming plane wave couple the gap-plasmon inside the slits.<sup>21</sup> ENZ are usually not considered in the context of IR sensors for a simple reason: the field enhancement they produce is exclusively located inside the material, making them *a priori* useless in this context.<sup>22-26</sup> Here we show that, by combining nanoslits and an ENZ material made of a doped semiconductor, it is possible to design simple plasmonics structures theoretically able to reach the most extreme values of the enhancement factor (typically  $10^7$ ) while extending the detection zone spatially. Finally, the resonance on which the response of the device is based is relatively large spectrally compared to usual plasmonic resonances and we show that the spectral range suited

<sup>a)</sup>Electronic mail: emmanuel.centeno@uca.fr

This is the author's peer reviewed, accepted manuscript. However, the online version of record will be different from this version once it has been copyedited and typeset.

PLEASE CITE THIS ARTICLE AS DOI: 10.1063/1.50070748

for detection can easily be changed by modifying the doping level of the semiconductor.

The periodic structure we consider consists in a periodic set of slits drilled in a metallic film on top of a ENZ material which is itself backed by a metallic substrate, shown Fig.1(a). It constitutes what is increasingly referred to as a metasurface. In this study, we consider gold for the metallic elements but similar results can be obtained with other noble metals or even doped semiconductors.<sup>27</sup> A poly(methyl methacrylate) (PMMA) film of thickness  $h_p$  is introduced in between the slits. Such materials presents several vibrational absorption peaks in the mid-IR range between 5 to 15  $\mu\text{m}$  ( $500\text{-}2000\text{ cm}^{-1}$ ). We use a Lorentz model for the relative permittivity of the PMMA layer whose absorption lines amplitudes and resonant frequencies are extracted from table 1 of reference<sup>28</sup>. The aspect ratio of the nanogaps is set to one in order to facilitate the practical realization of such structure – so that  $f/h_r = 1$ . In the following, the period and the ENZ film thickness are kept constant with  $d = 0.6\mu\text{m}$  and  $g = 1.6\mu\text{m}$ . The metasurface is illuminated in normal incidence by a p-polarized plane wave, which corresponds to a magnetic field along the slits. The electromagnetic properties of the structures are simulated with a home-made electromagnetic code based on the rigorous coupled-wave analysis method.<sup>29</sup> The optical absorption of the structure is deduced from the reflectance  $R$  by  $A = 1 - R$  since the electromagnetic waves are not transmitted through the back mirror. The gold permittivity is given by a Drude model whose validity extends to the IR frequency range:  $\epsilon_{Au}(\omega) = \epsilon_\infty - \omega_p^2/(\omega^2 - i\gamma\omega)$  with  $\epsilon_\infty = 5.97$ ,  $\omega_p = 1.33 \times 10^{16}\text{ rad s}^{-1}$  and  $\gamma = 10^{14}\text{ rad s}^{-1}$ .<sup>30</sup> The absorption spectra show a very large contrast for 10 nm nanogaps filled with a 2 nm thick PMMA layer, Fig.1(b). The optical absorption for the same structure shows a flat and weak response when the optical losses of the PMMA are artificially suppressed (by removing the oscillator terms of the Lorentz model). In the following, the terms *with* and *without* refer to the case of a PMMA layer with and without the Lorentz oscillator terms. This indicates that the metasurface selectively detects the vibrational peaks of the molecules in the slits. The SEIRA signal is computed with the relative reflectance change,  $\Delta R/R_0 = (R_{with} - R_{without})/R_0$ . Here,  $R_0$  is the reflection coefficient of the reference gold mirror which is almost constant (around 98%) since the MIR frequency range is well above the plasma frequency of gold. For example, at 8.65  $\mu\text{m}$ ,  $\Delta R/R_0$  varies between 15 % to 65 % when the PMMA thickness increases from 1 nm to 10 nm, Fig.2(a). The SEIRA signal is well above the noise level even for a 1 nm thick PMMA layer. These values are 4 orders of magnitude higher than that observed for a 10 nm thick bare PMMA layer on top of the reference mirror, Fig.2(b). For comparison, a reflectance difference of 15-20 % is typically reached with nano-antennas or nanogap-based structures when much thicker films of molecules of several dozens of nanometers are considered.<sup>14,16,31</sup>

The material optical dispersion of the metal and of the molecules prevents an efficient detection over the whole molecule fingerprint range. Since the SEIRA signal is usually obtained as a perturbation of a plasmonic resonance that

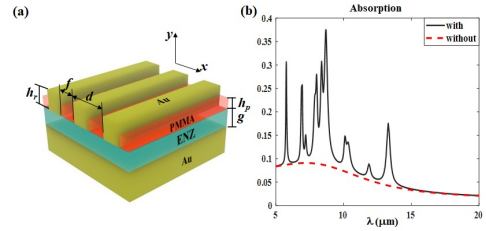


FIG. 1. (a) Diagram of the metasurface. In the following the thickness of the ENZ material is  $g = 1.6\mu\text{m}$ , the period of the slits is  $d = 0.6\mu\text{m}$  and the aspect ratio of the nanogaps  $f/h_r = 1$ . (b) Absorption spectra with a 2 nm thick PMMA film and for  $f = 10\text{ nm}$  slit width, with and without the optical absorption associated to the oscillator terms of the Lorentz model.

strongly depends on the structural parameters, the geometry has typically to be scaled to match with the targeted IR range<sup>4,15,32</sup>. Here, the fact that the structure presents a broad resonance without the molecules allows us to enhance the SEIRA signal at any frequency without bringing any change to the geometry of the structure. The comparison of the SEIRA signal (Fig.2(a)) with the extension coefficient of the PMMA (Fig.2(c)) demonstrates indeed that with the structure, the SEIRA signal accurately reproduces the vibrational fingerprints of the PMMA.

We emphasize that the resonance mechanism identified for such a structure and which leads to perfect absorption at any wavelength cannot alone explain such a large SEIRA improvement.<sup>15,33-35</sup> The presence of the ENZ material is crucial for the enhancement of the IR vibrational absorption. The calculations show that the reflectance difference is indeed optimal when the permittivity of the material is close to zero, Fig.3(a). Moreover, although the optical losses within the ENZ material are often detrimental to the proper operation of ENZ metamaterials, here the SEIRA signal degrades only when the ENZ layer presents a large optical absorption, as shown Fig.3(b).

The first reason explaining how the ENZ layer enhances the SEIRA detection concerns the coupling of the incident light with the mode supported by the slit. It has been experimentally demonstrated that such a bulk ENZ medium is able to assist the transmission through subwavelength channels.<sup>21</sup> The detailed theoretical analysis proves that the ENZ layer increases the coupling between the fundamental slit mode identified as a gap-plasmon mode and the free-space modes. Secondly, this better coupling is also accompanied by the enhancement of the amplitude of the gap-plasmon mode.<sup>36</sup> However, the high contrast for the SEIRA signal we obtained whatever of the thickness of the PMMA introduced in the slits suggests that an additional mechanisms takes place in the presence of the ENZ spacer. To elucidate this point, we have calculated the gap-plasmon modes inside the structure with the eigen-solver of COMSOL Multiphysics software (Stockholm, Sweden). Bloch boundary conditions and perfectly matched layer have been implemented. We have

This is the author's peer reviewed, accepted manuscript. However, the online version of record will be different from this version once it has been copyedited and typeset.

PLEASE CITE THIS ARTICLE AS DOI: 10.1063/5.0070748

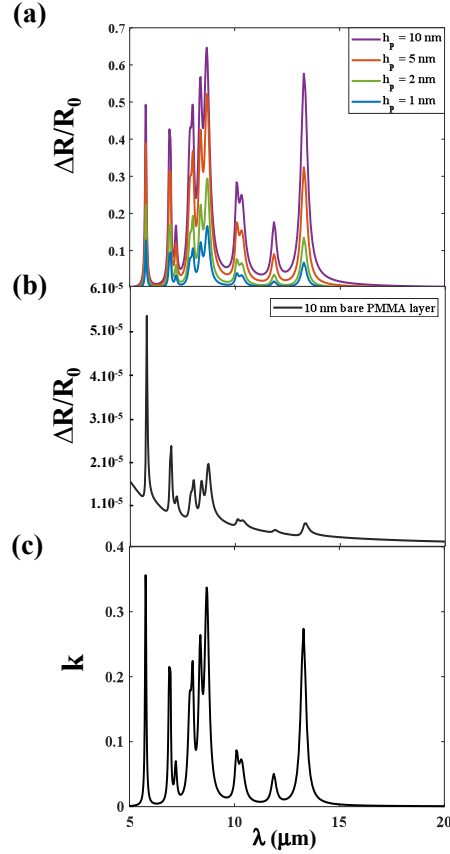


FIG. 2. (a) Relative change in reflectance for an increasingly thick PMMA layer as a function of the wavelength for the structure. (b) Relative reflectance for a 10 nm thick PMMA layer on top of the gold substrate. (c) Imaginary part ( $k$ ) of the refractive index of PMMA as a function of the wavelength showing that the fingerprint of PMMA can actually be retrieved using the proposed design.

found that the ENZ material strongly impacts the electromagnetic field of the gap-plasmon mode. The  $x$ -component of the electric field is particularly influenced by the presence of an ENZ medium surrounding the slit filled with air, as shown Fig.4. With air, the electric field is inhomogeneously distributed inside the slits. It is enhanced at the edges and rapidly decreases in the core of the slit, Fig.4(a). With an ENZ medium at both sides of the slits, the  $E_x$  field becomes completely homogeneous within the slit and the electric field presents parallel lines just like what occurs in the case of an infinite capacitor, Fig.4(b). This behavior is almost preserved

3

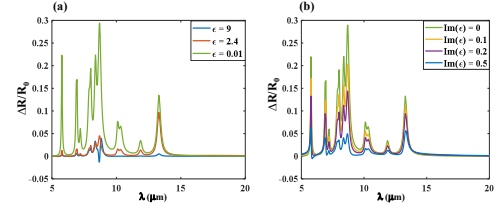


FIG. 3. Relative change in the reflectance spectrum calculated for a 2 nm thick PMMA layer and for 10 nm slits. (a) for an ENZ material of varying real part of the permittivity and neglecting optical losses. (b) for an ENZ material characterized by real part of 0.01 and an increasing imaginary part for the permittivity.

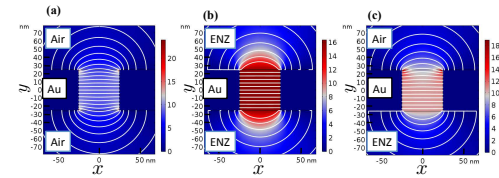


FIG. 4. Modulus of the  $x$ -component of the normalized electric field for 50 nm slits filled with air, when the slit is respectively surrounded by air (a), by an ENZ medium (b) and with air and ENZ medium (c). The permittivity of the ENZ medium is equal to 0.01. The electric field lines are represented in white. The respective complex resonant wavelengths in  $\mu\text{m}$  are  $8.9+2.1i$ ,  $7.1+1i$  and  $8.0+1.5i$ .

in an asymmetric situation with air on one side and an ENZ medium on the other one, Fig.4(c). To quantify the homogeneity of the electric field within the slit, we have computed the spatial average of the norm of the gradient of the modulus of electric field normalized to the modulus of electric field:  $\rho = \frac{1}{S_{\text{slit}}} \iint S_{\text{slit}} \|\nabla|E|\|/|E| dx dy$ . When the slit is surrounded by air,  $\rho = 12 \mu\text{m}^{-1}$ , while  $\rho = 0.3 \mu\text{m}^{-1}$  with the ENZ external medium. These values confirm that the electric field quickly varies within the slit when it is surrounded with air while it is uniform with the ENZ material outside. In the asymmetric configuration, with both air and ENZ external media,  $\rho = 6 \mu\text{m}^{-1}$  indicating that the electric field presents mixed characteristics, being uniform in the lower half of the slit and slightly inhomogeneous near the interface with air. Consequently, a molecule feels almost the same exalted electric field whatever its position within the slit leading to both to an enhancement of the field and to a much larger detection volume, thus explaining the large increase in the SEIRA signal in the presence of an ENZ material.

For the practical implementation, we consider a doped semiconductor as the ENZ material. Semiconductors are versatile materials for plasmonics since their doping allows to emulate a metal in the mid-IR range.<sup>27,37</sup> Here, we propose to rely on n-doped InAsSb for the spacer whose permittivity is

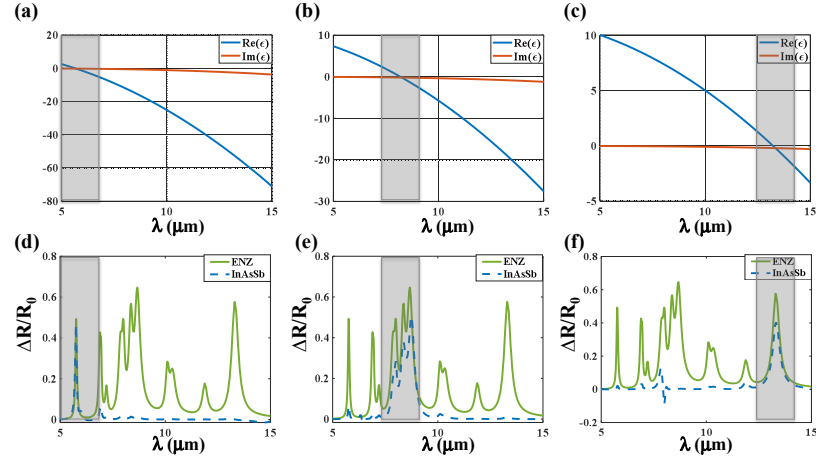


FIG. 5. (a-c) real and imaginary parts of the permittivity for an InAsSb doped spacer. (d-f) Reflectance difference spectra for a non-dispersive ENZ material (with  $\epsilon = 0.01$ ) and for an InAsSb doped spacer. The thickness of the PMMA layer is 10 nm and the slit size is 10 nm. The gray zone corresponds to the ENZ frequency range.

described by a Drude-like model:

$$\epsilon_{sc} = \epsilon_{\infty} \left( 1 - \frac{\omega_p^2}{\omega^2 + i\omega\Gamma} \right), \quad (1)$$

where  $\epsilon_{\infty} = 12.6$  is the high frequency permittivity,  $\Gamma = 10^{13}$   $\text{rad s}^{-1}$  is the damping constant and  $\omega_p = \sqrt{ne^2/\epsilon_0\epsilon_{\infty}m^*}$  the angular plasma frequency with the free-electron effective mass  $m^*$ . The InAsSb permittivity is close to zero when the angular frequency approaches  $\omega_p$ . Since the doping level modifies the carrier density  $n$ , it is possible to design an ENZ medium operating around any targeted vibrational absorption range of the molecules. By varying the carrier density between  $4.5 \times 10^{18} \text{ cm}^{-3}$  and  $6 \times 10^{19} \text{ cm}^{-3}$  the ENZ band shifts from the first to the last absorption lines of the PMMA when Fig.5(a-c). Here  $\omega_p$  takes the values:  $1.18 \times 10^{15} \text{ rad s}^{-1}$ ,  $7.54 \times 10^{14} \text{ rad s}^{-1}$ ,  $4.83 \times 10^{14} \text{ rad s}^{-1}$  for the respective Fig. 5 (a), (b) and (c). The relative reflectance change calculated for the doped InAsSb shows that the SEIRA signal is high and very close to the ideal non-dispersive ENZ material, Fig.5(d-f). According to the results of Fig.3(b), the efficiency of the structure is marginally affected by the optical losses intrinsic to the InAsSb semiconductor.

As discussed in the introduction, the reduction of the detection volume leads to an enhancement of the electric field and consequently an increase of the EF, but systematically decreases the amount of the molecules concerned by this local enhancement. This is why the SEIRA detectors based on actual plasmonic structures do not present both large EF and high SEIRA signal-noise ratio. The SEIRA enhancement factor (EF) is defined as  $(I_{SEIRA}/I_0) \times (A_0/A_{SEIRA})$  where  $I_{SEIRA}$  is the enhanced and  $I_0$  the unenhanced signal strength. In

our case,  $I_{SEIRA}$  and  $I_0$  correspond to the relative reflectance respectively calculated for the same PMMA thickness with the structure and for the bare PMMA on top of the back mirror. Furthermore,  $A_{SEIRA}$  and  $A_0$  denote the areas (volumes) covered (filled) with molecules in SEIRA or reference measurements<sup>4</sup>. In our case,  $\text{EF} = (I_{SEIRA}/I_0) \times (d/f)$ . We calculate the EF as a function of the slit sizes for the PMMA absorption line  $8.65 \mu\text{m}$  ( $1100 \text{ cm}^{-1}$ ) and for a 2 nm PMMA layer Fig.6. When the InAsSb is properly doped to behave as an ENZ medium around this frequency, the EF reaches  $1.6 \times 10^5$  for a 50 nm slit and up to  $1.4 \times 10^7$  for a 5 nm slit. These values are close to those obtained for the non-dispersive ENZ material free of optical losses ( $\text{EF} = 2.35 \times 10^7$  for  $f = 5$  nm). This extreme EF can be explained by the unique properties of the ENZ-based IR detector. First, The presence of the ENZ spacer increases the coupling with the gap plasmon mode supported by the slit. We observe a huge enhancement of the electric field intensity, about  $|E/E_0|^2 = 12000$  for slits of 10 nm width illuminated by a plane wave in normal incidence, Fig.6. Secondly, the almost uniform spatial distribution of the electric field allows to maximize the effective detection volume.

In summary, we have proposed a design for a SEIRA sensor based on nanoslits whose field concentration capabilities are enhanced by the presence of an Epsilon Near Zero material, leading to an extremen enhancement factor up to  $10^7$ , similar to what has been obtained with bowtie shaped antennas. Our design however presents a much larger detection zone located inside the slits whose width ranges between 5 nm to 50 nm. Such a design should allow to escape the trade-off between the enhancement factor and the signal to noise ratio. Furthermore, the use of a doped semiconductor as an ENZ provides

This is the author's peer reviewed, accepted manuscript. However, the online version of record will be different from this version once it has been copyedited and typeset.

PLEASE CITE THIS ARTICLE AS DOI: 10.1063/1.50070748

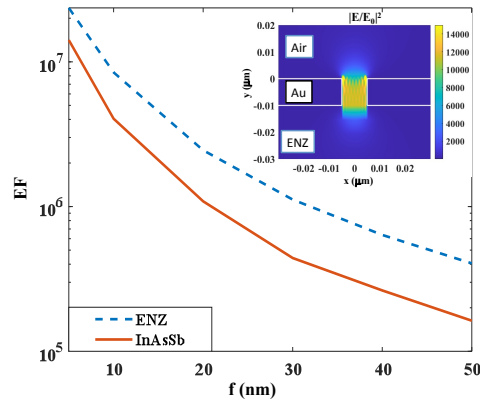


FIG. 6. SEIRA enhancement factor (EF) calculated for the  $8.65 \mu\text{m}$  absorption peak as a function of the slit size  $f$  for a non-dispersive ENZ material (with  $\epsilon = 0.01$ ) and for an InAsSb doped spacer. The thickness of the PMMA layer is 2 nm. The inset represents the enhancement of the electric field for  $f = 10 \text{ nm}$ .

an efficient and cheap solution to detect the whole vibrational resonances of molecules without modifying the geometry.

In this work, the ENZ is used to tailor the response of a plasmonic resonator, and not for its intrinsic properties. We think that the design principles which can be deduced from the present study could well be applied to many other similar situations, improving the efficiency of plasmonic IR sensors by using ENZ materials to reshape plasmonic resonances.

#### ACKNOWLEDGMENTS

We wish to acknowledge the support received from the Agence Nationale de la Recherche of the French government through the program investissements d'avenir IDEX-0001 CAP 20-25 and the IMoBS3 Laboratory of Excellence (ANR-10-LABX-0016). Antoine Moreau is an Academy CAP 20-25 chair holder.

#### DATA AVAILABILITY STATEMENT

The data that support the findings of this study are available from the corresponding author upon reasonable request.

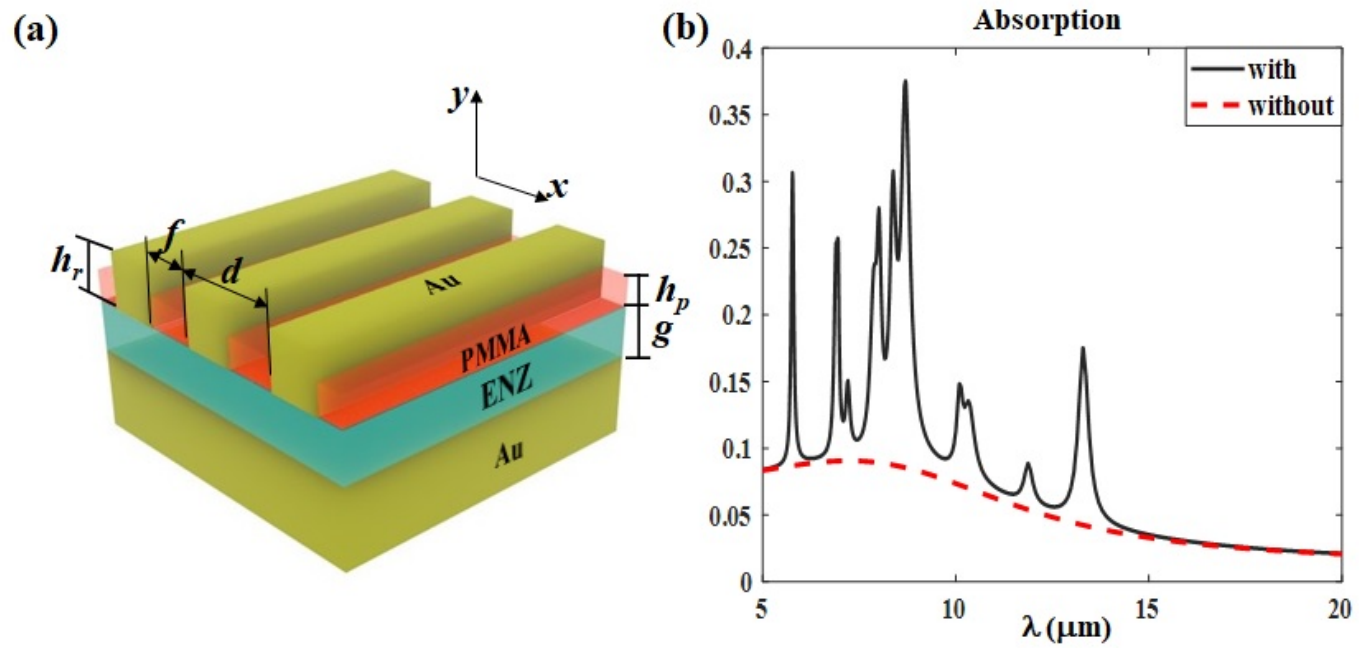
#### REFERENCES

<sup>1</sup>P. R. Griffiths and J. A. De Haseth, *Fourier transform infrared spectrometry*, Vol. 171 (John Wiley & Sons, 2007).

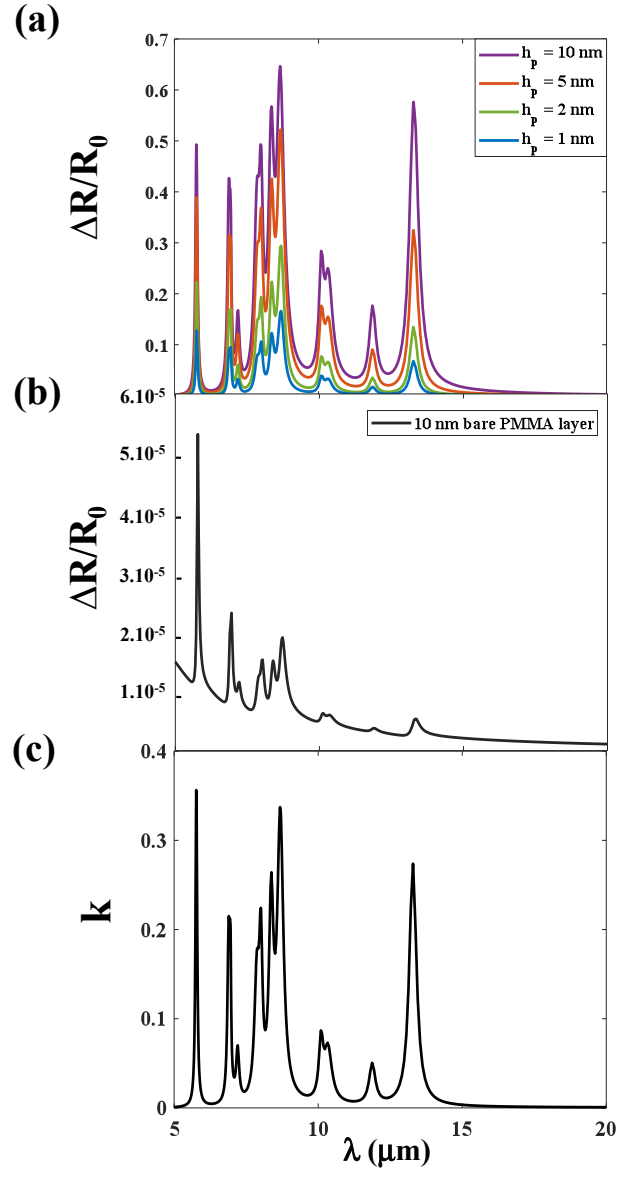
- <sup>2</sup>A. Hartstein, J. Kirtley, and J. Tsang, *Physical Review Letters* **45**, 201 (1980).
- <sup>3</sup>M. Osawa, *Topics Appl. Phys* **81**, 163 (2001).
- <sup>4</sup>F. Neubrech, C. Huck, K. Weber, A. Pucci, and H. Giessen, *Chemical reviews* **117**, 5110 (2017).
- <sup>5</sup>F. Neubrech, A. Pucci, T. W. Cornelius, S. Karim, A. García-Etxarri, and J. Aizpurua, *Physical review letters* **101**, 157403 (2008).
- <sup>6</sup>E. Cubukcu, S. Zhang, Y.-S. Park, G. Bartal, and X. Zhang, *Applied Physics Letters* **95**, 043113 (2009).
- <sup>7</sup>L. V. Brown, K. Zhao, N. King, H. Sobhani, P. Nordlander, and N. J. Halas, *Journal of the American Chemical Society* **135**, 3688 (2013).
- <sup>8</sup>F. B. Barho, F. Gonzalez-Posada, M.-J. Milla-Rodrigo, M. Bomers, L. Cerutti, and T. Taliercio, *Optics express* **24**, 16175 (2016).
- <sup>9</sup>C. Huck, F. Neubrech, J. Vogt, A. Toma, D. Gerbert, J. Katzmann, T. Härtling, and A. Pucci, *ACS Nano* **8**, 4908 (2014).
- <sup>10</sup>L. Dong, X. Yang, C. Zhang, B. Cerjan, L. Zhou, M. L. Tseng, Y. Zhang, A. Alabastri, P. Nordlander, and N. J. Halas, *Nano letters* **17**, 5768 (2017).
- <sup>11</sup>J. Srajer, A. Schwaighofer, G. Ramer, S. Rotter, B. Guenay, A. Kriegner, W. Knoll, B. Lendl, and C. Nowak, *Nanoscale* **6**, 127 (2014).
- <sup>12</sup>A. Cattoni, P. Ghenuche, A.-M. Haghiri-Gosnet, D. Decanini, J. Chen, J.-L. Pelouard, and S. Collin, *Nano letters* **11**, 3557 (2011).
- <sup>13</sup>X. Chen, C. Ciraci, D. R. Smith, and S.-H. Oh, *Nano letters* **15**, 107 (2015).
- <sup>14</sup>D. Yoo, D. A. Mohr, F. Vidal-Codina, A. John-Herpin, M. Jo, S. Kim, J. Matson, J. D. Caldwell, H. Jeon, N.-C. Nguyen, *et al.*, *Nano letters* **18**, 1930 (2018).
- <sup>15</sup>A. Fabas, H. El Ouazzani, J.-P. Hugonin, C. Dupuis, R. Haidar, J.-J. Greffet, and P. Bouchon, *Optics Express* **28**, 39595 (2020).
- <sup>16</sup>C. Huck, J. Vogt, M. Sendner, D. Hengstler, F. Neubrech, and A. Pucci, *ACS Photonics* **2**, 1489 (2015).
- <sup>17</sup>M. Dechaux, P.-H. Tichit, C. Ciraci, J. Benedicto, R. Polles, E. Centeno, D. R. Smith, and A. Moreau, *Physical Review B* **93**, 045413 (2016).
- <sup>18</sup>A. Moreau, C. Ciraci, J. J. Mock, R. T. Hill, Q. Wang, B. J. Wiley, A. Chilkoti, and D. R. Smith, *Nature* **492**, 86 (2012).
- <sup>19</sup>F. Ding, Y. Yang, R. A. Deshpande, and S. I. Bozhevolnyi, *Nanophotonics* **7**, 1129 (2018).
- <sup>20</sup>R. Smaali, F. Omeis, E. Centeno, T. Taliercio, F. Gonzalez-Posada, and L. Cerutti, *Physical Review B* **100**, 041302 (2019).
- <sup>21</sup>D. Adams, S. Inampudi, T. Ribaudou, D. Slocum, S. Vangala, N. Kuhta, W. Goodhue, V. A. Podolskiy, and D. Wasserman, *Physical review letters* **107**, 133901 (2011).
- <sup>22</sup>D. Berreman, *Physical Review* **130**, 2193 (1963).
- <sup>23</sup>S. Vassant, J.-P. Hugonin, F. Marquier, and J.-J. Greffet, *Optics express* **20**, 23971 (2012).
- <sup>24</sup>S. Campione, I. Brener, and F. Marquier, *Physical Review B* **91**, 121408 (2015).
- <sup>25</sup>D. Yoo, F. de León-Pérez, M. Pelton, I.-H. Lee, D. A. Mohr, M. B. Raschke, J. D. Caldwell, L. Martín-Moreno, and S.-H. Oh, *Nature Photonics* **15**, 125 (2021).
- <sup>26</sup>T. G. Folland, G. Lu, A. Brunz, J. R. Nolen, M. Tadjer, and J. D. Caldwell, *ACS Photonics* **7**, 614 (2020).
- <sup>27</sup>T. Taliercio and P. Biagioni, *Nanophotonics* **8**, 949 (2019).
- <sup>28</sup>S. Jitian and I. Bratu, *AIP Conference Proceedings* **1425**, 26 (2012), <https://aip.scitation.org/doi/pdf/10.1063/1.3681958>.
- <sup>29</sup>T. Weiss, G. Granet, N. A. Gippius, S. G. Tikhodeev, and H. Giessen, *Optics express* **17**, 8051 (2009).
- <sup>30</sup>D. P. Edward and I. Palik, *Handbook of optical constants of solids* (1985).
- <sup>31</sup>R. Adato, A. A. Yanik, J. J. Amsden, D. L. Kaplan, F. G. Omenetto, M. K. Hong, S. Erramilli, and H. Altug, *Proceedings of the National Academy of Sciences* **106**, 19227 (2009).
- <sup>32</sup>K. Weber, M. L. Nesterov, T. Weiss, M. Scherer, M. Hentschel, J. Vogt, C. Huck, W. Li, M. Dressel, H. Giessen, *et al.*, *ACS Photonics* **4**, 45 (2017).
- <sup>33</sup>R. Smaali, F. Omeis, A. Moreau, T. Taliercio, and E. Centeno, *Scientific reports* **6**, 1 (2016).
- <sup>34</sup>P. Chevalier, P. Bouchon, R. Haidar, and F. Pardo, *Applied Physics Letters* **105**, 071110 (2014).
- <sup>35</sup>A. P. Hibbins, J. R. Sambles, C. R. Lawrence, and J. R. Brown, *Physical review letters* **92**, 143904 (2004).
- <sup>36</sup>S. Inampudi, D. Adams, T. Ribaudou, D. Slocum, S. Vangala, W. Goodhue, D. Wasserman, and V. Podolskiy, *Physical Review B* **89**, 125119 (2014).
- <sup>37</sup>Y. Zhong, S. D. Malagari, T. Hamilton, and D. M. Wasserman, *Journal of Nanophotonics* **9**, 093791 (2015).

This is the author's peer reviewed, accepted manuscript. However, the online version of record will be different from this version once it has been copyedited and typeset.

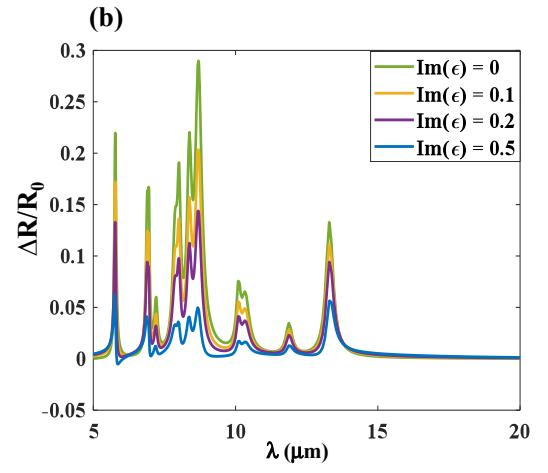
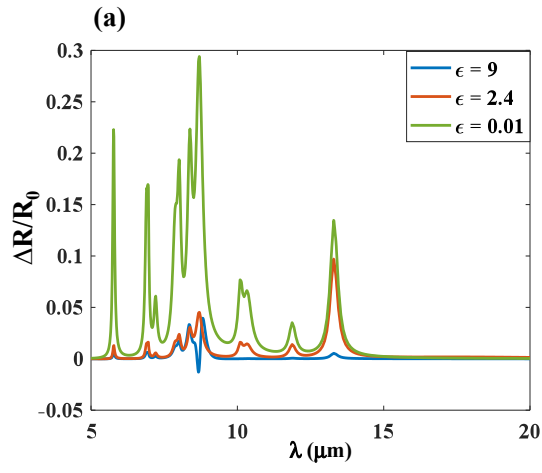
PLEASE CITE THIS ARTICLE AS DOI: 10.1063/5.0070748



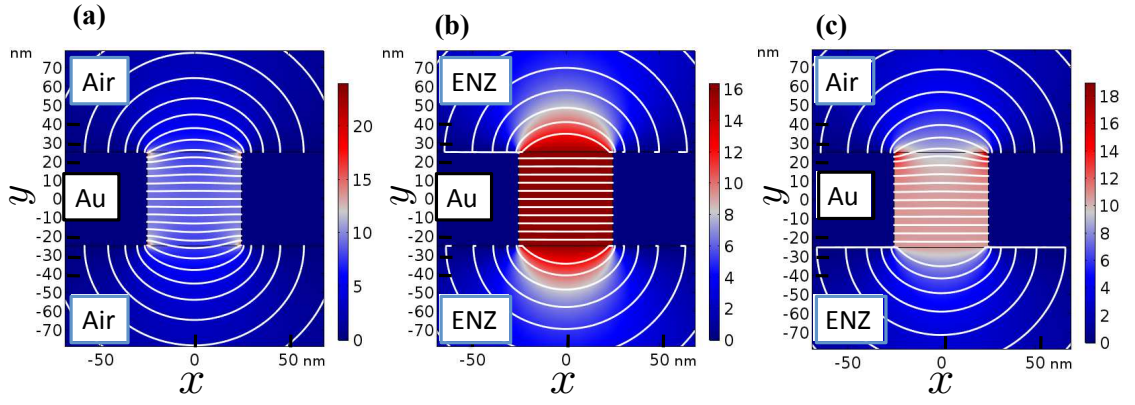
This is the author's peer reviewed, accepted manuscript. However, the online version of record will be different from this version once it has been copyedited and typeset.  
 PLEASE CITE THIS ARTICLE AS DOI: 10.1063/1.50070748



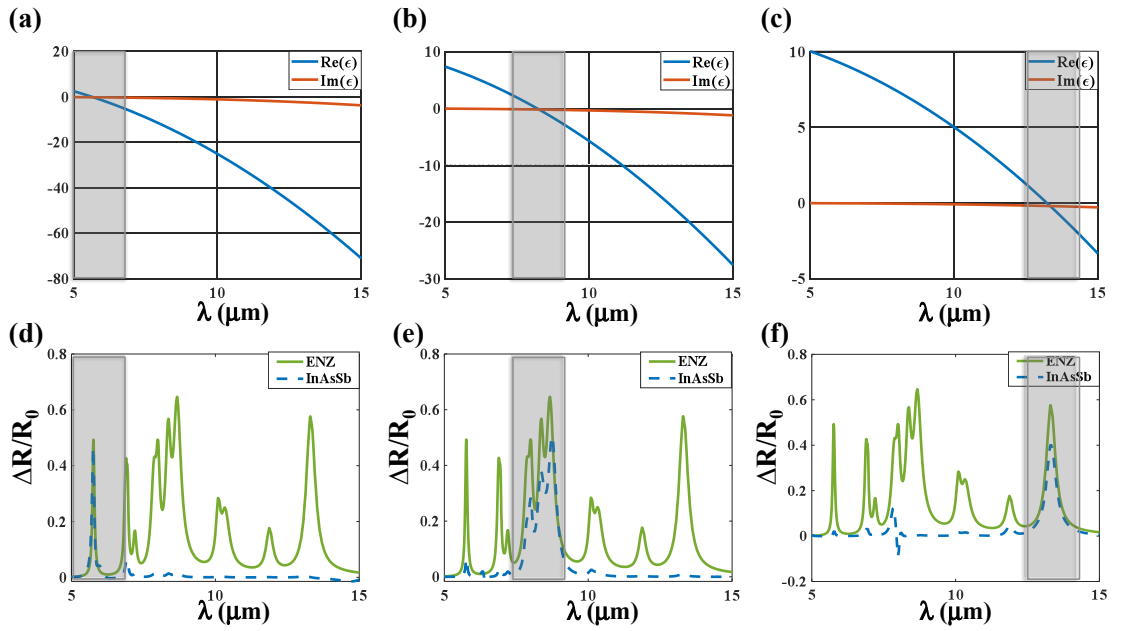
This is the author's peer reviewed, accepted manuscript. However, the online version of record will be different from this version once it has been copyedited and typeset.  
 PLEASE CITE THIS ARTICLE AS DOI: 10.1063/1.50070748



This is the author's peer reviewed, accepted manuscript. However, the online version of record will be different from this version once it has been copyedited and typeset.  
 PLEASE CITE THIS ARTICLE AS DOI: 10.1063/1.50070748



This is the author's peer reviewed, accepted manuscript. However, the online version of record will be different from this version once it has been copyedited and typeset.  
 PLEASE CITE THIS ARTICLE AS DOI: 10.1063/1.50070748



This is the author's peer reviewed, accepted manuscript. However, the online version of record will be different from this version once it has been copyedited and typeset.

PLEASE CITE THIS ARTICLE AS DOI: 10.1063/1.50070748

